



Evaluating the biosusceptibility of natural stone as an supporting tool to prevent Cultural Heritage biodeterioration

L. Dias^{1,2}, V. Pires¹, F. Sitzia^{1,2}, C. Lisci¹, A. Candeias^{1,3}, A. T. Caldeira^{1,3}, J. Mirão^{1,2,a} 

¹ HERCULES Laboratory and IN2PAST–Associated Laboratory for Research and Innovation in Heritage, Arts, Sustainability and Territory, University of Évora, Évora, Portugal

² Geosciences Department, Sciences and Technology School, University of Évora, Évora, Portugal

³ Chemistry and Biochemistry Department, Sciences and Technology School, University of Évora, Évora, Portugal

Received: 7 September 2022 / Accepted: 10 June 2023

© The Author(s) 2023

Abstract Biodeterioration of construction materials is still a major challenge that conservator-restorers face, especially in historic monuments with high cultural value. Natural stone is highly susceptible to deterioration through physical, chemical, and biological ways, whereas biological proliferation may potentiate both chemical and physical deterioration. The composition of the colonizers and their proliferation are highly dependent on climatic parameters like temperature and humidity, which are distinct from place to place. The present work proposes the execution of an innovative methodology that enables the determination of the susceptibility of natural stone to biocolonization, a parameter denominated as biosusceptibility. The study aims to contribute to the creation of models by predicting their deterioration even before the objects' manufacture, promoting the sustainability of one of the most valuable natural resources. The methodology proposed here was performed on limestones, marbles and slates—exploited in the Portuguese territory—by using colonizing strains typically found on stones exposed to the Mediterranean climate. The results have demonstrated that the stones with higher porosity are less susceptible to epilithic colonization and, consequently, with a moderate alteration of their aesthetic appearance. However, the metabolic activity determined in these stones is higher, which indicates that biocolonization will cause more severe damage to their structure in the future. The first significant changes on the stones' matrix were assessed one year after the inoculation, using cutting-edge technology of 3D surface micro-reconstruction. Due to its relevance in natural stone deterioration processes, the inclusion of the biosusceptibility information in technical brochures is strongly encouraged.

1 Introduction

Natural stone, due to its excellent physical–chemical and aesthetic properties, has always been one of the most preferred natural construction materials of the most prestigious buildings, monuments, or artefacts. Its exploitation is traditionally associated with European countries, which continues to be a reference model in this sector, where it combines competence with creativity, investing in new technologies to improve the quality of its products and services. To maintain its competitiveness in this field, it is important to create additional tools that enable the development of predictability models, namely through building information modelling (BIM) protocols. On the other hand, it is of utmost importance to apply these supporting tools to preserve stones that are part of our heritage [1].

Despite the physical and chemical properties that characterize natural stone as a building material par excellence, it is a substrate susceptible to deterioration mechanisms like any other natural material, triggered either by extrinsic [2–5] and/or intrinsic factors [6–8]. The current bibliography refers to several studies conducted in laboratories, which relate physical (e.g. UV light, temperature, humidity) [9–11] and chemical (e.g. SO₂ action) [10, 12] factors to deterioration of stone. However, there has been a lack of laboratory studies that enable to mimic the effects of deterioration on stone mediated by microorganisms, a process denominated biodeterioration. The biodeterioration of natural stone, a subject that was neglected for several years, is now considered one of the major factors leading to its physical and chemical deterioration (Fig. 1), either by the action of the filamentous hyphae [13–15] or products excreted by the colonizers (i.e. pigments, acids) [16, 17]. The development of biofilms on the surface of the stone also promotes an evident aesthetic alteration [16, 18–21], denigrating eventual sculpted details and natural patterns of the stone itself, namely colour and texture.

Biosusceptibility or bioreceptivity was defined by Guillitte in 1995 [22], and it refers to the susceptibility of a material to biological deterioration caused by macro- or microorganisms such as fungi, algae, lichens and bacteria. Natural stone is a material susceptible to biological colonization due to its porous nature and the presence of organic compounds that can act as nutrients for microbial

^a e-mail: jmirao@uevora.pt (corresponding author)

Fig. 1 Aesthetic and structural alterations of a historic sculpture made of limestone from the sixteenth century, co-promoted by microbial activity [16]



growth [23–25]. Currently, fungi are the microorganisms that are considered to have the most physical decohesion effects on these materials, since their development can lead to cracking and spalling [26, 27]. Fungi hyphae can penetrate deep into natural stone, which can weaken the structure of the stone and make it more susceptible to further deterioration. The formation of biofilms by fungi can also trap moisture and nutrients that can accelerate the growth of other microorganisms.

The formation of biofilms is a process that can naturally occur relatively quickly, and their development strongly depends on the substrate characteristics and the environmental conditions. This study aims to encourage the inclusion, in catalogues and brochures, of the parameter biosusceptibility, which describes the resistance of stones to biological deterioration.

2 Materials and methods

2.1 Selection of the lithotypes

Different lithotypes currently exploited in the Portuguese territory took part in this study, namely limestones, marbles, and slate. The denomination of each selected lithotype and its relevant characteristics are presented in Table 1. The stones were selected based on their high potential for building applications and conservation-restoration interventions.

2.2 Obtaining the microbial isolates

Three different eukaryotic strains were selected to inoculate the stones. These fungi were previously isolated from natural stone exposed outdoor and exhibiting aesthetic alterations [16, 29]. The strains obtained (Table 2) were characterized and sequenced through Sanger method and using the Basic Local Alignment Search Tool (BLAST) at the National Center for Biotechnology Information (NCBI) database. The strains *Cladosporium* sp. and *Phoma* sp. belong to the phylum Ascomycota, and the strain *Schizophyllum* sp. belongs to the phylum Basidiomycota, whose have been extensively associated with the colonization of stone-constructed buildings and artefacts [20, 21, 29–31].

Fresh cultures of these isolates were prepared in slants using Malt Extract Agar culture medium (malt extract, glucose, and peptone) and grown for 4 days at 28 °C. The cells were therefore placed in a sterilized physiological saline medium (0.9% w/v), obtaining a solution with 2×10^7 cells/mL. For this purpose, the cells were counted in a Neubauer chamber supported by an optical microscope.

2.3 Preparation of the natural stone mock-ups

Natural stone blocks were supplied by companies of the ornamental stone sector. The mock-ups used to execute the experiment were prepared ($1.5 \times 1.5 \times 1.5$ cm) with a DISPLAN-TS precision saw and therefore autoclaved in polypropylene bags at 110 °C for 25 min to be able to control the further development of the cells.

2.4 Experimental setup

After sterilization, the specimens were inoculated with 1×10^6 cells of each strain in each stone mock-up, depositing several drops on its surface. After the inoculation, the stone mock-ups were placed in an Aralab Fitoclima 600 climatic chamber at constant temperature and relative humidity of 28 °C and 90%, respectively. One mock-up of each lithotype was incubated without cell

Table 1 Description of the lithotypes used for the biosusceptibility assessment

Commercial name	Petrography and classification according to Folk [28]	Chemical composition	Open porosity (%)
Rosal Dunas (limestone)	Carbonate rock with recognizable depositional grain-supported texture. It is characterized by a strong presence of bioclasts, peloids and some oolites (bio-ool-pelsparite)	CaO 55.73%; MgO 1.35%; SiO ₂ 0.69%; K ₂ O 0.11%; Na ₂ O 0.09%; Al ₂ O ₃ 0.06%; Fe ₂ O ₃ 0.05%; TiO ₂ 0.02%; LOI* 43.70%	12.3
Moca creme (limestone)	Carbonate rock with recognizable depositional grain-supported texture. It is characterized by a strong presence of bioclasts, peloids and some oolites (bio-ool-pelsparite)	CaO 55.63%; MgO 1.24%; SiO ₂ 0.75%; K ₂ O 0.10%; Na ₂ O 0.08%; Al ₂ O ₃ 0.09%; Fe ₂ O ₃ 0.07%; TiO ₂ 0.01%; LOI 43.44%	8.5
Alpinina (limestone)	Limestone rock with micritic mud-supported matrix. Presence of subparallel recrystallized sparite veins with openings from 0.1 mm up to 5 mm and variable spacing (Pelbiomicrite-sparite)	CaO 54.81%; MgO 1.20%; SiO ₂ 0.89%; K ₂ O 0.11%; Na ₂ O 0.07%; Al ₂ O ₃ 0.10%; Fe ₂ O ₃ 0.05%; TiO ₂ 0.01%; LOI 43.79%	0.7
Crema JPL (marble)	Calcitic marble with homeoblastic granoblastic interlobate texture. Strongly isotropic and oriented texture with MGS = 1.5 mm. Grain boundary shape (GBS) mainly curved and secondarily straight	CaO 55.81%; MgO 1.71%; SiO ₂ 1.21%; K ₂ O 0.15%; Na ₂ O 0.08%; Al ₂ O ₃ 0.19%; Fe ₂ O ₃ 0.43%; TiO ₂ 0.01%; LOI 42.66%	0.2
Rosa JPL (marble)	Calcitic marble with homeoblastic semi-polygonal granoblastic texture. Strongly oriented and isotropic with MGS = 2 mm. GBS of mainly straight and secondarily curved type	CaO 55.22%; MgO 1.52%; SiO ₂ 1.10%; K ₂ O 0.17%; Na ₂ O 0.09%; Al ₂ O ₃ 0.09%; Fe ₂ O ₃ 0.26%; TiO ₂ 0.01%; LOI 43.27%	0.2
Brecha St. António (limestone)	Bioclastic dolomite-calcite limestone, with sparite and recrystallized zones (Biosparite)	CaO 51.54%; MgO 1.12%; SiO ₂ 3.12%; K ₂ O 0.16%; Na ₂ O 0.05%; Al ₂ O ₃ 1.41%; Fe ₂ O ₃ 2.34%; TiO ₂ 0.07%; LOI 40.98%	4.7
Ardósia Valongo (slate)	Very fine-grained metamorphic rock with porphyrooid-lepidoblastic texture	CaO 0.44%; MgO 3.72%; SiO ₂ 45.05%; K ₂ O 3.96%; Na ₂ O 1.42%; Al ₂ O ₃ 31.71%; Fe ₂ O ₃ 8.60%; TiO ₂ 1.43%; LOI 5.81%	1.2

*LOI: Loss of ignition at 1060 °C

inoculation to function as a control specimen. The assays were performed in triplicate. Every week, 50 µL of Malt Extract culture medium was added to the mock-ups by depositing it as drops.

2.5 Analytical methodology

2.5.1 Macroscopic and microscopic recording

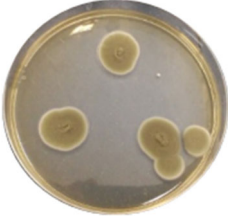
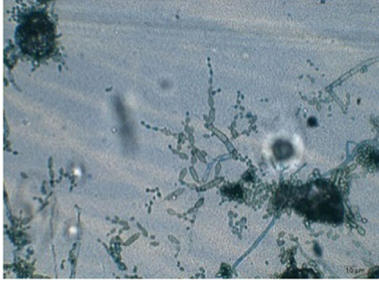



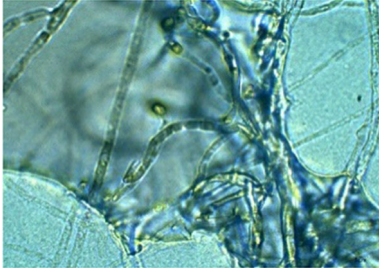
The macroscopic and microscopic appearance of the stone mock-ups and the viability of the grown cells were evaluated at 15, 30, and 60 days after inoculation. The stone mock-ups were observed under a HIROX-01 digital microscope coupled to a NPS Confocal White Light system to record the macroscopic aspect and to perform 3D surface micro-modelling. The 3D micro-modelling using the NPS Confocal White Light System was performed on a 1 × 1 mm surface area, scanning 1000 lines with 200 µm s⁻¹ scanning speed. In each period, the stone mock-ups were removed from the climatic chamber under aseptic conditions and observed in the digital microscope.

2.5.2 Cell viability

Cell viability was determined through the reduction of 3-(4,5-dimethylthiazol-2-yl)-2,5-diphenyltetrazolium bromide (MTT), previously described by Mosman [32]. This is a colourimetric method used to quantify the viable cells present in a solution, which is based on the reduction of MTT (yellow-coloured substance) to formazan (blue-coloured substance), through the action of dehydrogenases. Thus, the metabolic activity of the cells is evaluated through the quantification of formazan, which concentration is directly proportional to the dehydrogenases' activity. In this case, the value of the metabolic activity index corresponds to the slope of each trend line. Higher slope values mean a higher cell viability index.

In each period, after observing the stone mock-ups in the digital microscope, they were placed in Falcon tubes with 3 mL of saline solution, where the cells were extracted for 24 h at 150 rpm.

Table 2 Characterization of the fungal isolates used for the biosusceptibility study

Macroscopic features	Microscopic features	Closest related type strain on basis of 18S rRNA gene and ITS
		<i>Cladosporium</i> sp.
		<i>Phoma</i> sp.
		<i>Schizophyllum</i> sp.

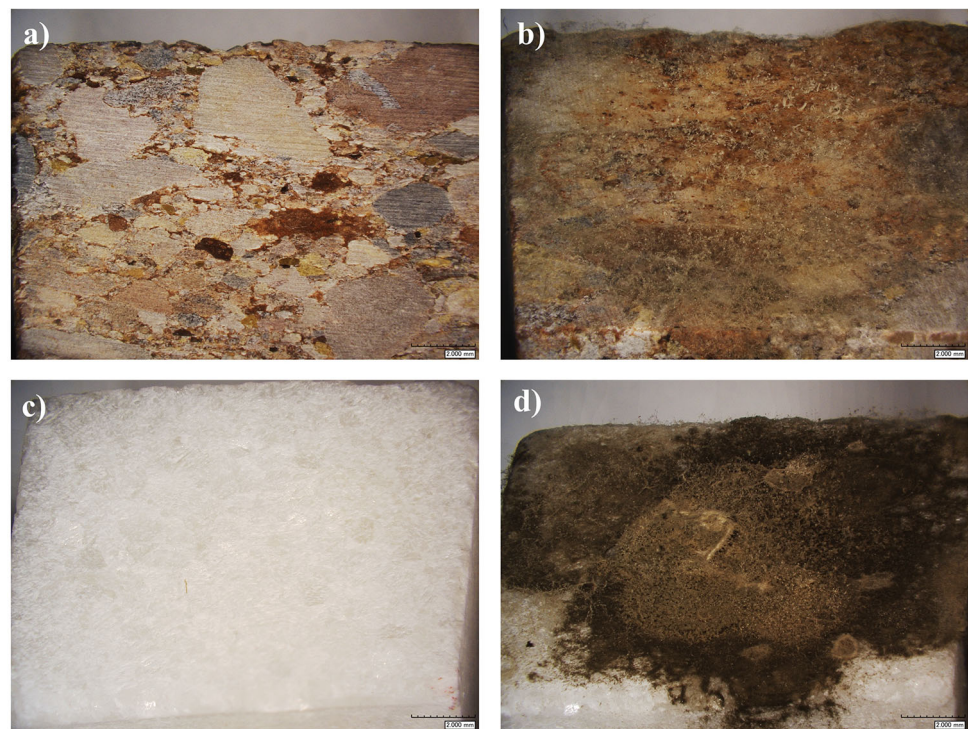
After the extraction, the solution obtained for each stone mock-up was transferred to Eppendorfs and kept at 4 °C overnight. The metabolic activity study was performed according to the procedure following described. 200 µL of solution was transferred to a microtube and 300 µL of MTT reagent (0.5 mg/mL) was added, followed by incubation for 4 h at 37 °C in the dark. After the incubation, the solution was centrifuged for 10 min at 10,000 rpm and the supernatant was discarded. 350 µL of DMSO/ethanol (1:1, v/v) was added to dissolve the purple formazan crystals, followed by new centrifugation for 10 min at 10,000 rpm. The absorbance was measured at 570 nm on a ThermoScientific MultiskanGo plate reader, using 200 µL of solution placed in a reading plate.

2.5.3 Colourimetry experiments and determination of C.F.U.

After 60 days of inoculation, the colour of all stone mock-ups was measured using a DataColor CheckPlusII portable spectrophotometer with a measuring aperture of 5 mm. The colour was determined at 3 different points on the inoculated surface by measuring the parameters of the CIELAB colour space. This measurement aims to determine the total difference in colour (by calculating the ΔE) of each lithotype caused by the biological colonization, using the formula: $\Delta E = ((\Delta L)^2 + (\Delta a)^2 + (\Delta b)^2)^{1/2}$, where $\Delta L = L^*_{t60days} - L^*_{t0days}$; $\Delta a = a^*_{t60days} - a^*_{t0days}$; $\Delta b = b^*_{t60days} - b^*_{t0days}$.

The colony forming units (C.F.U.) of each solution were also determined in this period. For this, 100 µL of each solution was inoculated by inclusion in Malt Extract Agar culture medium placed in a Petri dish. After solidification, the plates were incubated for 5 days at 28 °C. This experiment was performed in triplicate.

Fig. 2 Aesthetic effects promoted by the inoculation of *Cladosporium* sp. on the surface of Brecha St. António at **a** t0d and **b** t60d, and Creme JPL at **c** t0d e **d** t60d



2.6 Assessment of structural alterations

The structural alterations of the stones were assessed 1 year after the inoculation using 3D surface micro-reconstruction technology. These surface reconstructions were performed using a Scanning Electron Microscope HITACHI S-3700N through the four quadrants of the backscattered electron (BSE) detector. The surface of each stone was analysed without any preparation step, operating the SEM at 20 keV accelerating voltage, 40 Pa chamber pressure, and 10 mm working distance. The 3D models were built and processed using the software MountainsMap® 7.

3 Results and discussion

The main scope of the present study is to contribute to the implementation of a tool that will enable the evaluation of a parameter that measures the resistance of natural stone against biodeterioration, denominated as biosusceptibility. To achieve it, three different microbial strains were applied to substrates that typically compose architectural projects, and their proliferation and effects were measured using a multi-analytical methodology.

3.1 Macroscopic and microscopic appearance

Photographic recording enabled to monitor the microbial growth and the aesthetic integrity of the stones. This was also performed for the control specimens, which remained unaltered during the experiments (data not shown). 15 days after the inoculation, it was already possible to observe microbial proliferation, indicating that the inoculated populations are settling and attaching to the surface of the stones. 60 days after the inoculation, an intense formation of biofilms was observed, especially in the metamorphic rocks (Fig. 2). This fact may be related with their low porosity and, consequently, low capacity to absorb moisture and nutrients [33], promoting a microbial proliferation that is essentially epilithic. This phase indicates that the inoculated population are likely adapted to the atmospheric conditions, as well as to the substrate where they are growing. The biofilm formation has a protective function, and it is a mechanism that assures the trap of nutrients. However, all stones demonstrated to be susceptible to microbial growth on the surface, as it became perceptible with the reconstructions obtained through confocal microscopy. The colour changed and the commercial finish was lost due to a change of texture (Fig. 3). This process known as biodeterioration involves several physical transformations that alter the appearance and properties of the stone. Besides some chemical transformations may also occur due to the release of pigments that can impart different hues to the stones' surface, in this case, it seems that the discolouration observed is essentially due to the colour of the microbial colonizers and their cell debris. Additionally, an increase in the roughness of natural stone surfaces may favor water and nutrient retention, leading to a cause-effect cycle. This was rapidly achieved on some lithotypes

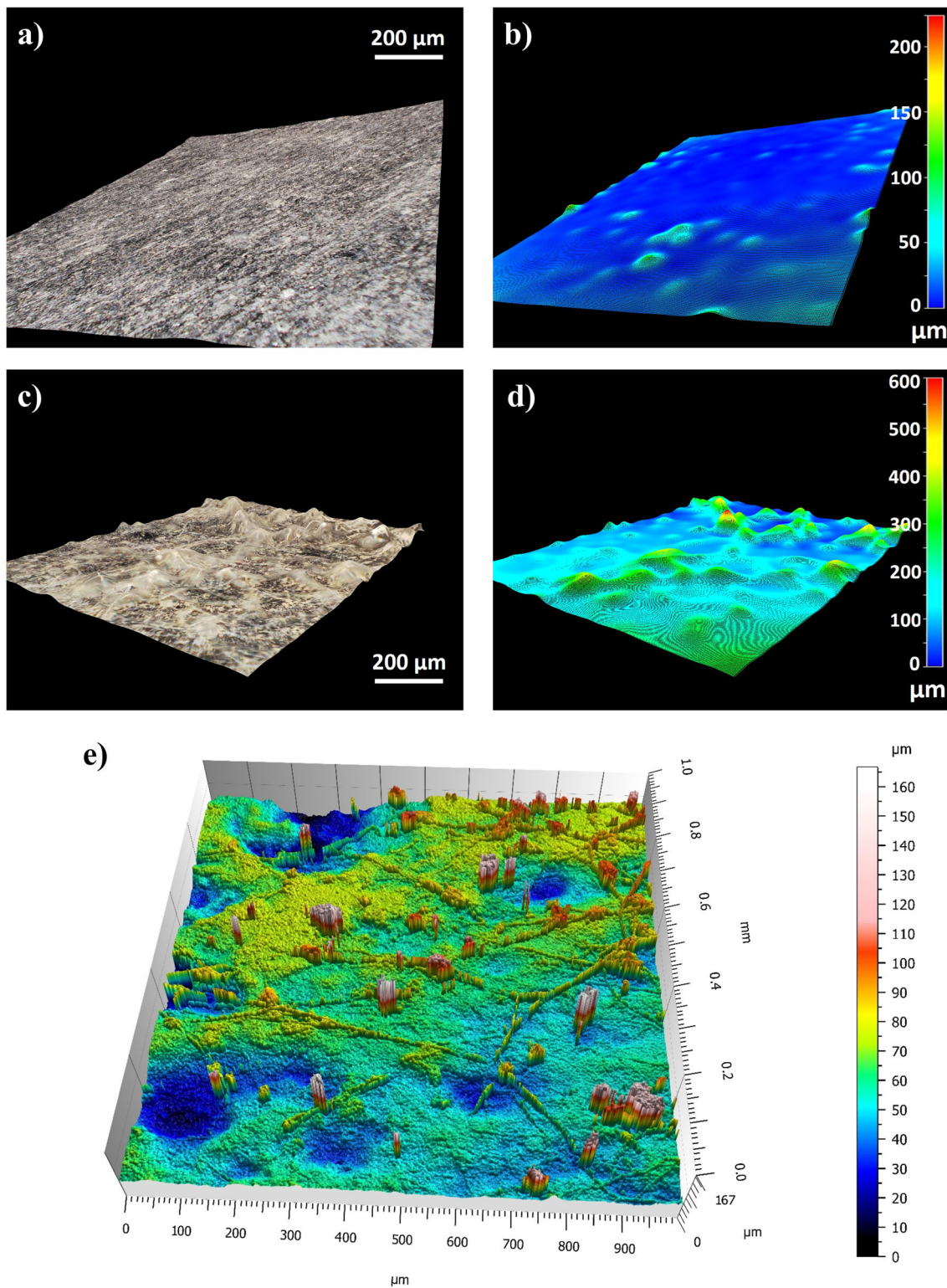


Fig. 3 Structural effects promoted by the inoculation of *Schizophyllum* sp. on the surface of Ardósia Valongo at **a, b** t0d and **c, d** t60d and Rosal Dunas at **e** t60d. Reconstructions were performed with NPS confocal white light system. The roughness increased significantly after the microorganisms' proliferation

since only 60 days were needed. Despite being a methodology that promotes accelerated growth of microorganisms, these effects will be unavoidably felt on these materials applied on exposed buildings or artefacts [24, 34, 35] if no intervention occurs to promote its preservation.

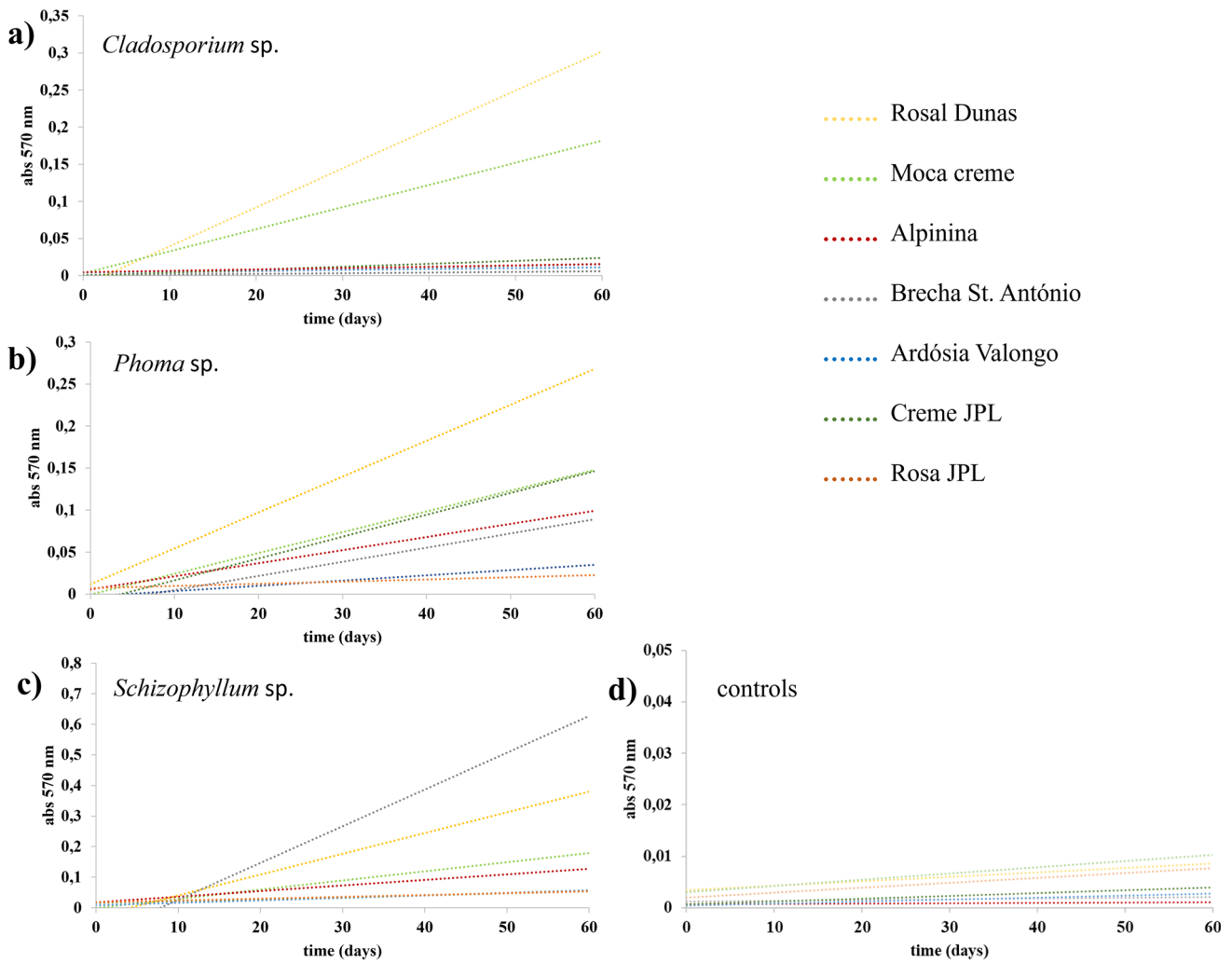


Fig. 4 Graphical representation of the metabolic activity of the cells from the different strains, proliferating on the surface of the stone mock-ups. **a** *Cladosporium* sp., **b** *Phoma* sp., **c** *Schizophyllum* sp., and **d** controls

Table 3 The microbial activity indexes were calculated until 60 days after the inoculation. The metabolic activity index is given through the slope of the corresponding trend line

Sample	<i>Cladosporium</i> sp.	<i>Phoma</i> sp.	<i>Schizophyllum</i> sp.	Controls
Rosal Dunas	5.2×10^{-3}	4.3×10^{-3}	6.8×10^{-3}	9.0×10^{-5}
Moca creme	3.0×10^{-3}	2.5×10^{-3}	3.0×10^{-3}	1.0×10^{-4}
Alpinina	2.0×10^{-4}	1.6×10^{-3}	1.8×10^{-3}	6.0×10^{-6}
Brecha St. António	9.0×10^{-5}	1.7×10^{-3}	1.2×10^{-2}	2.0×10^{-5}
Ardósia Valongo	1.0×10^{-4}	6.0×10^{-4}	8.0×10^{-4}	4.0×10^{-5}
Creme JPL	4.0×10^{-4}	2.6×10^{-3}	6.0×10^{-4}	6.0×10^{-5}
Rosa JPL	2.0×10^{-4}	3.0×10^{-4}	6.0×10^{-4}	1.0×10^{-4}

3.2 Metabolic activity and structural alteration

The MTT assay has enabled to determine in which lithotypes have acted a higher metabolic activity [29]. Unlike the biofilms’ formation previously discussed, the lithotypes that demonstrated a higher metabolic activity index were Rosal Dunas, Moca Crème and Brecha St. António (Fig. 4 and Table 3), which are characterized to be limestones with high open porosity (Table 1). These results suggest that these lithotypes are more susceptible to endolithic colonization. Due to this physical property, porous stones have a greater capacity to retain moisture and nutrients in their pores, which triggers cell proliferation within their matrixes. An endolithic proliferation by fungi will imply the sporulation of hyphae [36] inside the pores of the stone. This expansion can cause the stone to crack or split, particularly if the stone has pre-existing fissures or weaknesses. In the worst scenarios, this expansion leads

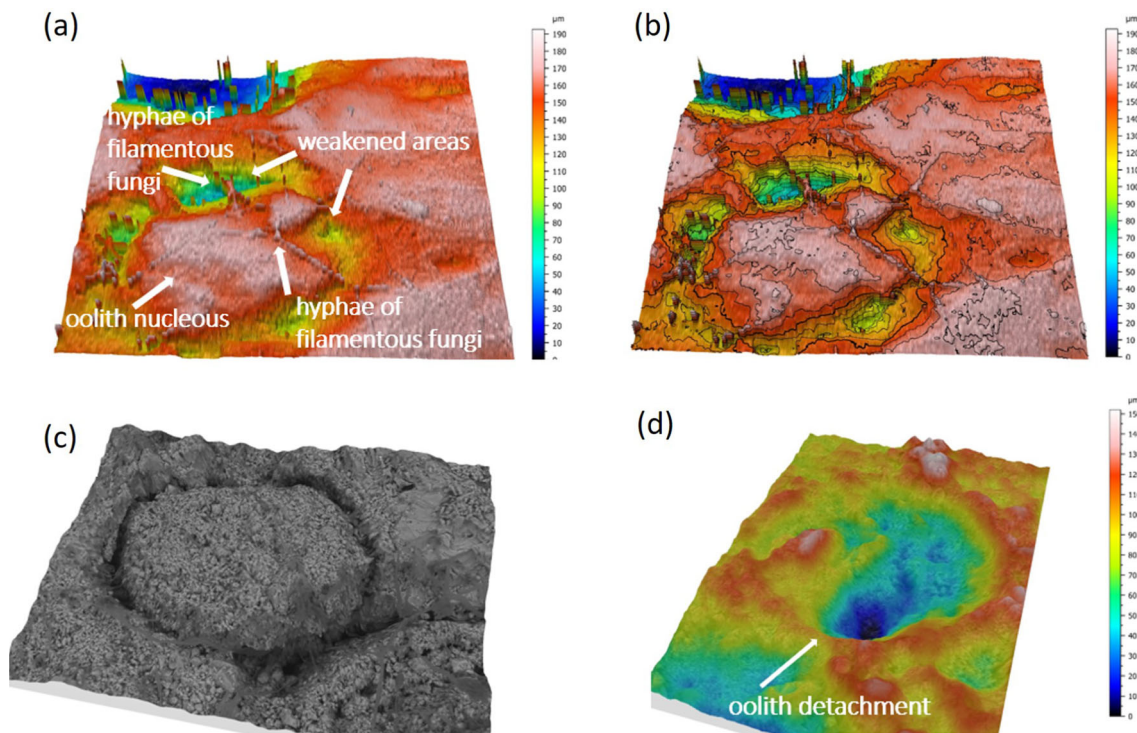


Fig. 5 Structural alterations caused by the development of *Schizophyllum* sp. on the surface of Rosal Dunas. 3D surface micro-reconstructions at (a, b, c) t60d and at (d) t360d through SEM and confocal microscopy, and the software MountainsMap[®] 7

to the disintegration of the stone [37, 38], leading to permanent loss of material which induces particular constraints on Cultural Heritage artworks. Consequently, in the long term, structural deterioration will be stronger in more porous lithotypes. The 3D surface micro-reconstructions have enabled a deep insight into the effects of stones' biocolonization. Rosal Dunas is a lithotype rich in oolites and peloids, which are small, spherical structures that form in shallow marine environments through the accumulation of calcium carbonate around a nucleus. In this stone, it was possible to assess the detachment of some oolites and peloids from the matrix of the stone since pits became visible on its surface (Fig. 5). This detachment was most likely mediated by the action of the filamentous fungi through cement deterioration that holds these structures. Nevertheless, more data are needed to investigate if the mechanism has involved chemical (e.g. dissolution through acids release) or/and physical (e.g. disruption by hyphae growth) processes. This was a short-term effect that completely changed the physical appearance of the surface of the stone, which made this lithotype not suitable for applications under specific conditions. The metabolic activity was also measured in non-inoculated stone mock-ups, which worked as a control for the experiment.

The execution of this methodology makes it possible to establish that the microbial proliferation on the surface of the stones is dependent not only on the substrate characteristics but also on the colonizing strain itself, which should be defined depending on which climate the stones will be settled [39, 40].

The C.F.U. were determined 60 days after the inoculation (Table 4). It was found that limestones have the highest C.F.U. values, most likely due to its greater capacity to retain moisture and nutrients, corroborating the results previously obtained. On the other hand, the colour measurements showed that the biological colonization impute a significant colour change on the surface of the stones, and the alteration of this physical parameter is more evident in the stones colonized by the strain *Cladosporium* sp.. This may be directly related to the greater capacity of this strain to colonize carbonate and silicate substrates in an epilithic way [41, 42].

4 Conclusions

Biocolonization plays a key role in stone deterioration, and a detailed understanding of the process is required. The application of the innovative methodology here presented enabled to determine which natural stone lithotypes would be most susceptible to biological colonization using microbial strains of the phyla Ascomycota and Basidiomycota. Regarding these colonizing strains, it was demonstrated that the stone lithotypes with a relatively high degree of open porosity are more susceptible to endolithic proliferation. In contrast, lithotypes with a lower degree of open porosity (whether carbonate or silicate) are more prone to the formation of biofilms on their surfaces. Besides less susceptibility to aesthetic alterations, endolithic colonization implies greater

Table 4 Total colour difference (ΔE) induced on the stones by each colonizing strain and C.F.U. determination, 60 days after the inoculation

Sample	<i>Cladosporium</i> sp.		<i>Phoma</i> sp.		<i>Schizophyllum</i> sp.	
	ΔE	C.F.U. (CFU/mL)	ΔE	C.F.U. (CFU/mL)	ΔE	C.F.U. (CFU/mL)
Rosal Dunas	13.03	2.9×10^5	11.58	1.1×10^6	6.68	4.6×10^4
Moca creme	34.38	1.8×10^7	20.49	1.5×10^7	19.22	1.8×10^7
Alpinina	37.28	2.9×10^6	24.66	1.6×10^7	24.57	1.7×10^7
Brecha St. António	15.57	3.0×10^5	6.35	8.8×10^6	10.57	2.1×10^7
Ardósia Valongo	14.44	7.5×10^6	9.73	1.5×10^7	5.84	1.8×10^7
Creme JPL	28.73	6.2×10^5	28.92	7.5×10^6	26.99	6.1×10^6
Rosa JPL	29.65	4.4×10^5	21.30	4.1×10^6	22.99	6.8×10^6

structural alterations of the stones' matrix, as it became demonstrated with the 3D surface micro-reconstructions. It was not clear at this point of the research if the chemical composition influences the proliferation of this type of microorganisms.

This study intends to contribute to a thoughtful consideration regarding the choice of the most suitable lithotypes in the execution of a particular architectural project, allowing relevant economic impacts on the natural stone value chain and leading to adjusted maintenance and conservation practices.

Encouraging the inclusion of "biosusceptibility", as a parameter defined by the susceptibility of a building material to biological colonization and deterioration, in product catalogues can promote the sustainable use of stone as a natural resource. This work has important applications in the preservation of cultural objects, as it identifies suitable materials for specific projects. The achievements of this study are a valuable contribution for industry associations, government agencies, and private companies, who should continue to discuss its implications. In addition, the need for sustainable solutions with antimicrobial potential is emphasized, which can lead to more effective preservation of these substrates over time.

Funding Open access funding provided by FCTIFCCN (b-on). The authors gratefully acknowledge the following funding sources: INOVSTONE4.0 (POCI-01-0247-FEDER-024535) co-financed by the European Union through the European Regional Development Fund ALENTEJO 2020, Fundação para a Ciência e a Tecnologia under the projects UIDB/04449/2020 and UIDP/04449/2020, and the project Sustainable Stone by Portugal - Valorization of Natural Stone for a digital, sustainable and qualified future, n° 40, proposal n° C644943391-00000051, co-financed by PRR - Recovery and Resilience Plan of the European Union (Next Generation EU).

Data Availability Statement This manuscript has associated data in a data repository. [Authors' comment: The datasets generated during and/or analysed during the current study are available from the corresponding author on reasonable request.]

Declarations

Conflict of interests The authors have no competing interests to declare that are relevant to the content of this article.

Open Access This article is licensed under a Creative Commons Attribution 4.0 International License, which permits use, sharing, adaptation, distribution and reproduction in any medium or format, as long as you give appropriate credit to the original author(s) and the source, provide a link to the Creative Commons licence, and indicate if changes were made. The images or other third party material in this article are included in the article's Creative Commons licence, unless indicated otherwise in a credit line to the material. If material is not included in the article's Creative Commons licence and your intended use is not permitted by statutory regulation or exceeds the permitted use, you will need to obtain permission directly from the copyright holder. To view a copy of this licence, visit <http://creativecommons.org/licenses/by/4.0/>.

References

1. F.J. López, P.M. Leronés, J. Llamas, J. Gómez-García-Bermejo, E. Zalama, Multimodal Technol Interact (2018). <https://doi.org/10.3390/mti2020021>
2. D.G. Kanellopoulou, P.G. Koutsoukos, in 10th International Symposium on the Conservation of Monuments in the Mediterranean Basin (Springer International Publishing, Cham, 2018). https://doi.org/10.1007/978-3-319-78093-1_36
3. O. Ortega-Morales, J.L. Montero-Muñoz, J.A. Baptista Neto, I.B. Beech, J. Sunner, C. Gaylarde, Int Biodeterior Biodegr (2019) <https://doi.org/10.1016/j.ibiod.2019.104734>
4. A. Dionísio, E. Martinho, J.S. Pozo-António, M.A. Sequeira Braga, M. Mendes, Constr Build Mater (2021) <https://doi.org/10.1016/j.conbuildmat.2021.122327>
5. C. Lisci, F. Sitzia, V. Pires, J. Mirão, J Build Pathol Rehabil (2022). <https://doi.org/10.1007/s41024-022-00196-9>
6. F. Nasri, A. Boumezbeur, D. Benavente, Bull Eng Geol Environ (2019). <https://doi.org/10.1007/s10064-018-1410-7>
7. R. Padilla-Ceniceros, J. Pacheco-Martínez, R.A. López-Doncel, E.E. Orenday-Tapia, Rev Mex Cien Geol (2017) <https://doi.org/10.22201/cgeo.20072902e.2017.2.466>
8. L. Dias, F. Sitzia, C. Lisci, L. Lopes, J. Mirão, Boletim de Minas. 54, 103–116 (2020) <http://hdl.handle.net/10174/29310>
9. D. Guilbert, S. Caluwaerts, K. Calle, N. van den Bossche, V. Cnudde, T. de Kock, Sci Total Environ (2019). <https://doi.org/10.1016/j.scitotenv.2019.04.344>

10. J.L. Parracha, G. Borsoi, R. Veiga, I. Flores-Colen, L. Nunes, A.R. Garcia, L.M. Ilharco, A. Dionísio, P. Faria, *Build Environ* (2021). <https://doi.org/10.1016/j.buildenv.2021.108151>
11. F. Sitzia, C. Lisci, J. Mirão, *Constr Build Mater* (2021). <https://doi.org/10.1016/j.conbuildmat.2021.124311>
12. V. Pires, L.G. Rosa, P.M. Amaral, A. Dionísio, J.A.R. Simão, *J Mater Civ Eng* (2022). [https://doi.org/10.1061/\(ASCE\)MT.1943-5533.0004223](https://doi.org/10.1061/(ASCE)MT.1943-5533.0004223)
13. L. Dias, T. Rosado, A. Candeias, J. Mirão, A.T. Caldeira, *Build Environ* (2020). <https://doi.org/10.1016/j.buildenv.2020.106934>
14. A.T. Caldeira, N. Schiavon, G. Mauran, C. Salvador, T. Rosado, J. Mirão, A. Candeias, *Coat* (2021). <https://doi.org/10.3390/coatings11020209>
15. T. Rosado, M. Silva, A. Galvão, J. Mirão, A. Candeias, A.T. Caldeira, *App Phys A* (2016). <https://doi.org/10.1007/s00339-016-0525-6>
16. L. Dias, T. Rosado, A. Candeias, J. Mirão, A.T. Caldeira, *J Cult Herit* (2020). <https://doi.org/10.1016/j.culher.2019.07.025>
17. T. Rosado, M. Gil, J. Mirão, A. Candeias, A.T. Caldeira, *Int Biodeter Biodegr* (2013). <https://doi.org/10.1016/j.ibiod.2013.06.013>
18. A.Z. Miller, N. Leal, L. Laiz, M.A. Rogerio-Candelera, R.J.C. Silva, A. Dionísio, M.F. Macedo, C. Saiz-Jimenez, *Geol Soc London Spec Publ* (2022). <https://doi.org/10.1144/SP331.6>
19. M.F. Macedo, A.Z. Miller, A. Dionísio, C. Saiz-Jimenez, *Microbiology* (2009). <https://doi.org/10.1099/mic.0.032508-0>
20. A.Z. Miller, L. Laiz, J.M. Gonzalez, A. Dionísio, M.F. Macedo, C. Saiz-Jimenez, *Sci Total Environ* (2008). <https://doi.org/10.1016/j.scitotenv.2008.06.066>
21. F. Cappitelli, P. Principi, R. Pedrazzani, L. Toniolo, C. Sorlini, *Sci Total Environ* (2007). <https://doi.org/10.1016/j.scitotenv.2007.06.022>
22. O. Guillitte, *Sci Total Environ* (1995). [https://doi.org/10.1016/0048-9697\(95\)04582-L](https://doi.org/10.1016/0048-9697(95)04582-L)
23. D. Pinna, in *Microorganisms in the Deterioration and Preservation of Cultural Heritage*, E. Joseph (Ed), Springer (2021) <https://doi.org/10.1007/978-3-030-69411-1>
24. X. Liu, R.J. Koestler, T. Warscheid, Y. Katayama, J. Gu, *Nat Sustain* (2020). <https://doi.org/10.1038/s41893-020-00602-5>
25. A.Z. Miller, P. Sanmartín, L. Pereira-Pardo, A. Dionísio, C. Saiz-Jimenez, M.F. Macedo, B. Prieto, *Sci Total Environ* (2012). <https://doi.org/10.1016/j.scitotenv.2012.03.026>
26. D. Isola, F. Bartoli, P. Meloni, G. Caneva, L. Zucconi, *Appl Sci* (2022). <https://doi.org/10.3390/app12042038>
27. A.P. Santo, O.A. Cuzman, D. Petrocchi, D. Pinna, T. Salvatici, B. Perito, *Appl Sci* (2021). <https://doi.org/10.3390/app11136163>
28. R.L. Folk, Practical petrographic classification of limestones. *Am Assoc Pet Geol Bull* (1959). <https://doi.org/10.1306/0BDA5C36-16BD-11D7-8645000102C1865D>
29. L. Dias, T. Rosado, A. Coelho, P. Barrulas, L. Lopes, P. Moita, A. Candeias, J. Mirão, A.T. Caldeira, *AIMS Microbiol* (2018). <https://doi.org/10.3934/microbiol.2018.4.594>
30. T. Rosado, L. Dias, M. Lança, C. Nogueira, R. Santos, M.R. Martins, A. Candeias, J. Mirão, A.T. Caldeira, *Microbiologyopen* (2020). <https://doi.org/10.1002/mbo3.1030>
31. A.C. Pinheiro, N. Mesquita, J. Trovão, F. Soares, I. Tiago, C. Coelho, H.P. Carvalho, F. Gil, L. Catarino, G. Piñar, A. Portugal, *J Cult Herit* (2018). <https://doi.org/10.1016/j.culher.2018.07.008>
32. T. Mosmann, *J Immunol Methods* (1983). [https://doi.org/10.1016/0022-1759\(83\)90303-4](https://doi.org/10.1016/0022-1759(83)90303-4)
33. C. Franzen, P.W. Mirwald, *Environ Geol* 4 (2004) <https://doi.org/10.1007/s00254-004-1040-1>
34. O. Salvadori, A.C. Municchia, *Open Conf Proc J* (2016). <https://doi.org/10.2174/2210289201607020039>
35. Y. Nuhoglu, E. Oguz, H. Uslu, A. Ozbek, B. Ipekoglu, I. Ocak, I. Hasenekoglu, *Sci Total Environ* (2006). <https://doi.org/10.1016/j.scitotenv.2005.06.034>
36. I.C. Senanayake, A.R. Rathnayaka, D.S. Marasinghe, M.S. Calabon, E. Gentekaki, H.B. Lee, V.G. Hurdeal, D. Pem, L.S. Dissanayake, S.N. Wijesinghe, D. Bundhun, T.T. Nguyen, I.D. Goonasekara, P.D. Abeywickrama, C.S. Bhunjun, R.S. Jayawardena, D.N. Wanasinghe, R. Jeewon, D.J. Bhat, M.M. Xiang, *Mycosphere* (2020). <https://doi.org/10.5943/mycosphere/11/1/20>
37. C.C. Gaylarde, J.A. Baptista-Neto, *Npj Mater Degrad* (2021). <https://doi.org/10.1038/s41529-021-00180-7>
38. J. Trovão, F. Gil, L. Catarino, F. Soares, I. Tiago, A. Portugal, *Int Biodeter Biodegr* (2020). <https://doi.org/10.1016/j.ibiod.2020.104933>
39. X. Ding, W. Lan, A. Yan, Y. Li, Y. Katayama, J.D. Gu, *J Environ Manage* (2022). <https://doi.org/10.1016/j.jenvman.2021.114041>
40. G. Zhang, C. Gong, J. Gu, Y. Katayama, T. Someya, J.D. Gu, *Int Biodeter Biodegr* (2019). <https://doi.org/10.1016/j.ibiod.2019.104723>
41. N.C. Silva, A.R. Madureira, M. Pintado, P.R. Moreira, *App Microbiol Biotechnol* (2022). <https://doi.org/10.1007/s00253-022-11957-4>
42. P. Gaylarde, C. Gaylarde, *Corros Rev* (2004). <https://doi.org/10.1515/CORRREV.2004.22.5-6.395>